JOURNAL OF GUIDANCE, CONTROL, AND DYNAMICS
Vol. 15, No. 5, September-October 1992

Active Member Bridge Feedback Control for Damping Augmentation

Gun-Shing Chen* and Boris J. Lurie†
Jet Propulsion Laboratory, California Institute of Technology, Pasadena, California 91109

An active damping augmentation approach using active members in a structural system is described. The problem of maximizing the vibration damping in a lightly damped structural system is considered using the analogy of impedance matching between the load and source impedances in an electrical network. The proposed active damping augmentation approach therefore consists of finding the desired active member impedances that maximize the vibration damping, and designing a feedback control in order to achieve desired active member impedances. This study uses a bridge feedback concept that feeds back a combination of signals from sensors of the axial force and relative velocity across the active member to realize the desired active member impedance. The proposed active damping augmentation approach and bridge feedback concept were demonstrated on a three-longeron softly suspended truss structure.

Introduction

THE complexity of structural vibration control is a function of the structure's dynamic characteristics, the input disturbances, and the system performance goal. Generally, the various approaches to controlling structural vibrations can be categorized as structural tuning, disturbance isolation, vibration damping augmentation, and active positioning control. Although the structural tuning is typically a passive design process, disturbance isolation and vibration damping augmentation can be implemented either passively, or actively, using feedback control. When the vibration control is only required for a limited number of discrete locations in a large structural system, it may be desirable to use active positioning control. On the other hand, when the objective of the vibration control is to attenuate responses over a large, continuous portion of the structure, such as the surface accuracy maintenance of a large aperture reflector, damping augmentation of the entire structure becomes a logical approach. This paper describes an application of the active damping augmentation approach to a truss-type structural system. Although there are many ways of applying external forces to damp out structural vibrations,[1] this paper focuses on the use of active truss members (or simply "active members" hereafter) that consist of built-in actuators and sensors for the purpose of feedback control.

In structural dynamics and mechanical vibration analyses, the concept of mechanical impedance is not new.[2-6] However, this concept has not often been used by practicing engineers. On the other hand, many analysis techniques using the electrical impedance concept have been developed and applied in the electrical network analyses. It is known, for example, that the dissipated (real) power in an electrical network can be maximized by matching the load impedance to the complex conjugate of the source impedance. By analogy, it is expected that the vibration damping (i.e., rate of energy dissipation) can be maximized by adjusting the active member impedance with respect to the load impedance facing the active member, i.e., the structure's mechanical impedance measured at the connecting interface to the active member. The proposed active damping augmentation approach is therefore to 1) find the desired active member impedance that maximizes the vibration damping, and 2) design the active member feedback control in order for its impedance to be as desired. In order for the system to be stable with any number of active members, the present design approach is limited to the consideration of positive real active member impedances only.

There are various ways of implementing the desired active member impedance using feedback techniques, e.g., pure velocity feedback or pure force feedback. In these cases, however, the desired impedance will also dictate the feedback loop transfer function. As a result, the requirement to implement the desired impedance will, as a rule, conflict with the robustness requirements to the loop transfer function. Furthermore, such impedance is likely to be sensitive to the active member's parameter variations. To overcome these difficulties, a bridge feedback concept, originally developed in communication engineering, is explored in this study. In communication engineering, and particularly in the feedback amplifier design,[7,8] bridge feedback refers to feeding back a combination of both voltage and current measured at the input of a feedback amplifier in order for the amplifier's input impedance to match the wave impedance of the connected electrical cable. By analogy, signals from collocated sensors of the axial force and relative velocity across an active member can be combined and fed back to its actuator to realize the desired active member impedance. In the following section, the proposed active damping augmentation approach and bridge feedback concept will be demonstrated on a three-longeron softly suspended truss structure.

Design Approach

Impedance Modeling

To draw a mechanical parallel to the techniques developed for the analysis of electrical networks, it is necessary to establish a correspondence between the variables and parameters of electrical and mechanical systems. Among several such conventions known in the literature, this paper employs the one comparing force with current and velocity with voltage. This particular type of analogy maps power into power, allows for simple mechanical interpretation of Kirchhoff's laws, and preserves the topology of schematics, electrical and mechanical, thus greatly simplifying the analysis of complicated high-order systems.[3,5,9]

Received Feb. 1, 1991; revision received Nov. 11, 1991; accepted for publication Nov. 27, 1991.

*Technical Group Leader, Applied Mechanics Technologies Section, Mail Stop 157-316. Member AIAA.

†Member Technical Staff, Guidance and Control Section, Mail Stop 198-326.

In the electrical network analysis, the input (or driving point) impedance is defined as the ratio of the Laplace transforms of the voltage and current measurements at the input port of an electrical circuit. Following the chosen analogy, the mechanical driving point impedance is hereby defined as the Laplace transform of the velocity-to-force ratio measured at a structural or mechanical element. Using this definition, the mechanical driving point impedances (or simply "impedances") of a mass, a spring, and a viscous damper are derived and listed in Table 1. Preservation of the connective topology of the electrical and mechanical systems is illustrated in Fig. 1.

To derive the equivalent electrical model of an active member, one can start from the underlying mechanism of the built-in piezoelectric actuator. When the actuator is in a stress-free state (i.e., unloaded), the actuator motion is entirely due to the piezoelectric motion (x_{fr}) which is the product of the effective piezoelectric coupling coefficient d_{eff} and applied voltage. When the actuator is loaded, the resulting actuator motion is determined by the actuator's inherent mechanical impedance and load impedance facing the actuator. Therefore, the equivalent electrical model of an active member will consist of an equivalent electromotive force (emf = $\dot{x}_{fr}$) in series with the inherent mechanical impedance Z_0 as shown in Fig. 2.

Using Kirchhoff's laws, the axial force and relative velocity across the active member can be easily calculated from the equivalent electrical network of Fig. 2 as

$$f = \dot{x}_{fr}/(Z_0 + Z_L) \tag{1}$$

and

$$\begin{aligned} \dot{x} &= f \cdot Z_L \\ &= \dot{x}_{fr} \cdot [Z_L/(Z_0 + Z_L)] \end{aligned} \tag{2}$$

In the following design analysis, the above relations are incorporated into a transfer function block as shown in Fig. 3.

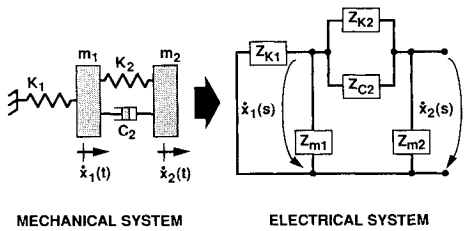

Fig. 1 Mechanical/electrical analogy.

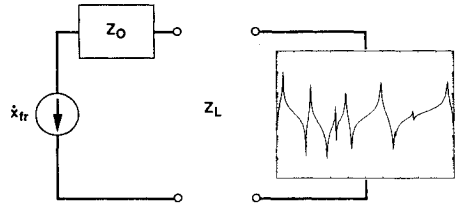

Fig. 2 Equivalent electrical model of active member.

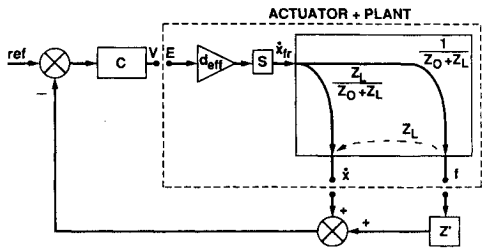

Fig. 3 Block diagram of bridge feedback control.

Table 1 Mechanical/electrical analogy[a]

Mechanical system		Electrical system	
Applied force, f Velocity, $\dot{x}$		Current, i Voltage, v	
Impedance = $\dot{x}(s)/f(s)$		Impedance = $v(s)/i(s)$	
Mass	$Z_m = 1/sm$	Capacitance	$Z_C = 1/sC$
Spring	$Z_k = s/k$	Inductance	$Z_L = sL$
Dashpot	$Z_c = 1/c$	Resistance	$Z_R = R$

[a]s: Laplace variable

Optimal Active Member Impedance

By analogy, maximizing the rate of energy dissipation in a structural system is equivalent to maximizing the dissipated (real) power in the equivalent network of Fig. 2. For a lightly damped structural system, load impedance facing the active member Z_L is almost imaginary. On the other hand, the active member impedance must have a real part to dissipate the energy. When the active member impedance is purely real, simple calculations show that the vibratory power dissipated by the active member is maximized when the active member impedance is equal to the magnitude of load impedance, i.e.,

$$Z(s) = Z_{opt} = |Z_L| \tag{3}$$

As illustrated in Fig. 2, $|Z_L|$ varies sharply with frequency and is typically sensitive to the parameter variations in a structural system. This and the conditions of positive, real $Z(s)$ make it impossible to implement the optimal impedance as specified in Eq. (3) over the entire frequency range. Instead, a suboptimal approach to implementing a simpler active member impedance function is proposed such that the dissipating power in the equivalent network of Fig. 2 is maximized in the average sense.[10] Such an impedance function can be as simple as a constant or piecewise linear function over the frequency range of interest. For example, in Ref. 11, the implementation of a piecewise linear active member impedance function was presented.

Bridge Feedback

In the active member bridge feedback design, signals from sensors of the axial force and relative velocity across the active member are combined and fed back to the active member's actuator as illustrated in Fig. 3. Transfer function block $Z'(s)$ in Fig. 3 determines how the signals of axial force and relative velocity can be combined in the feedback path. From the Appendix, the resulting impedance of the active member with bridge feedback is

$$Z(s) = Z_0(s) \cdot [(1 + T_0)/(1 + T_\infty)] \tag{4}$$

where T_0 and T_∞ are the return ratios of cases in which the active member is rigidly constrained (i.e., $Z_L = 0$) and free to expand (i.e., $Z_L = \infty$), respectively. The return ratio (loop transfer function) is defined as the ratio of return signal to input signal taken with the opposite sign, i.e., $T = -v/E$ in Fig. 3. When the active member is rigidly constrained, relations illustrated in Fig. 3 give $f = E \cdot d_{eff} \cdot s/Z_0$ and $\dot{x} = 0$. The return ratio T_0 is then

$$T_0 = \frac{d_{eff}}{Z_0(s)} \cdot s \cdot Z'(s) \cdot C(s) \tag{5}$$

where $C(s)$ represents the compensator transfer function. Following the same procedure, when the active member is free to expand, Fig. 3 gives $f = 0$, $\dot{x} = \dot{x}_{fr} = E \cdot d_{eff} \cdot s$ and return ratio as

$$T_\infty = d_{eff} \cdot s \cdot C(s) \tag{6}$$

When the magnitude of the compensator gain coefficient $|C(s)|$ is sufficiently large such that the magnitudes of the return ratios $|T_0|$ and $|T_\infty|$ of Eqs. (5) and (6) are much greater than unity, Eq. (4) can be approximated by

$$Z(s) \simeq Z_0(s) \cdot (T_0/T_\infty) \tag{7}$$

Substituting Eqs. (5) and (6) into Eq. (7) yields

$$Z(s) \simeq Z'(s) \tag{8}$$

As a result, when the feedback is sufficiently large, the impedance of the active member with bridge feedback can be completely defined by the transfer function block $Z'(s)$ in the feedback path. As evidenced in Eq. (8), the advantages of the bridge feedback are that 1) the compensator design, and subsequently the desired loop transfer function, does not interfere with the realization of desired active member impedance; and 2) the desired active member impedances can be implemented precisely despite the active member's parameter uncertainty affecting its inherent mechanical impedance $Z_0(s)$.

Truss Experiments

Test Structure and Active Members

To validate the approach in this paper, laboratory experiments were performed on a three-longeron, 13-bay truss structure made of removable aluminum truss members and threaded aluminum joints (Fig. 4). This test structure spanned 3.96 m (13 ft) from end to end and weighed 5.91 kg (13 lb). The active member used in this experiment, Fig 5, was a 203.2 mm (8 in.) long, 25.4-mm- (1-in.-) diam stainless steel thin-walled tube with a built-in eddy-current displacement sensor measuring the member axial length changes, and a piezoelectric actuator exerting the control forces. A load cell was incorporated in series with the active member to measure the induced member axial force. Detailed descriptions of the active member can be found in Refs. 12 and 13. The actuator and sensor parameters are summarized in Table 2. Two active members were incorporated in the test structure, one at the upper longeron location of the fifth bay (member no. 5) and the other at the tenth bay (member no. 30) as shown in Fig. 6. In addition to the active member's built-in sensors, the test structure was also instrumented with six highly sensitive QA-1400 accelerometers such that damping performance could be demonstrated at the very low end of the dynamic range, i.e., peak resonant response in the order of 0.001 g (1 g = 9.8 m/s^2).

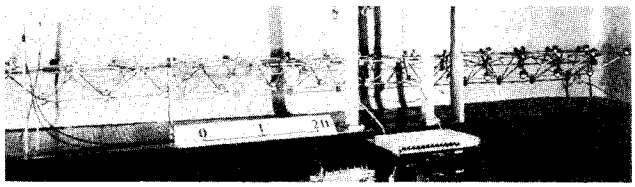

Fig. 4 Test structure.

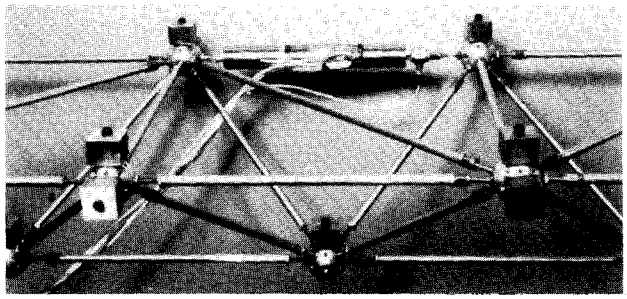

Fig. 5 Active member.

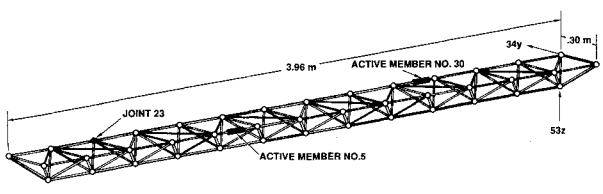

Fig. 6 Test structure dimensions and active member locations.

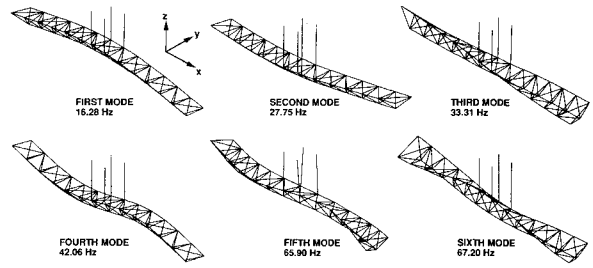

Fig. 7 Predicted normal modes of test structure.

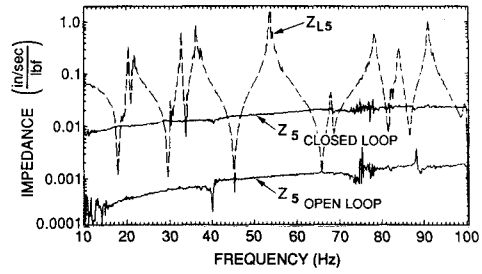

Fig. 8 Comparison of active member no. 5 impedances and its load impedance.

Table 2 Active member properties

Effective stiffness, k_{eff}	26.3 × 10^6 N/m
Effective piezoelectric constant, d_{eff}	54 × 10^{-9} m/V
Load cell sensitivity	11.24 × 10^{-3} V/N
Displacement sensor sensitivity	0.1 V/micron

To simulate the unconstrained in-space operation, the test structure was softly suspended at the central bay location. The suspension system consisted of four precompressed helical springs such that the intended low suspension frequencies, ranging from 0.13 to 1.37 Hz as measured, can be achieved without incurring large static deflections in helical springs. Analytical analyses showed no discrepancy in modal behavior of a completely unconstrained and softly suspended test structures. Modal behavior of the softly suspended test structure is shown in Fig. 7 up to the sixth mode. An independently suspended mini-shaker was connected to the test structure's second/third bay joint (joint no. 23 as shown in Fig. 6) to serve as a disturbance input.

Constant Active Member Impedance Synthesis and Realization

The bridge feedback signal processing and the compensator used in this experiment were implemented in analog circuitry. The relative velocity across the active member required for the bridge feedback was estimated from the relative displacement sensor output using an analog differentiator rolling off near 800 Hz.

As described earlier, to maximize the vibration damping, the active member impedance should be of specific value. After examining the measured load impedance facing each active member in the frequency range up to 100 Hz (e.g., Fig.

8 for active member no. 5), it was decided to synthesize the active member impedance to be real and constant that emulates the dynamic behavior of a viscous damper. Since the signal processing is ac coupled, the active member statically remained unaffected and the desirable static stiffness was preserved.

To realize the desired active member impedance via bridge feedback, the goal of the compensator design is to maximize the feedback over the frequency bandwidth as large as possible. It is known that the feedback available is limited by the slope steepness of the loop transfer function. From the Bode phase-gain relations,[7,8] however, a steeper slope in the loop transfer function will increase the loop phase lag and subsequently reduce the stability margin. Therefore, the feedback available is limited by the desired system stability margin.

Since the desired impedance of active member with bridge feedback is chosen to be real and constant, the transfer function Z' in the feedback path must be a constant according to Eq. (8). Because no phase lag is introduced by this constant, the allowable compensator of phase lag (i.e., phase margin minus 180 deg) is therefore completely determined by the loop phase margin. A typical value of phase margin, for example, is 30 deg. To account for the possibility of 180-deg phase shift due to the unmodeled structural resonances within the feedback bandwidth, additional phase margin of 90 deg is considered in the compensator design. The resulting phase margin is therefore 30 deg + 90 deg, i.e., 120 deg. While maximizing the feedback, the Bode phase-gain relations[7,8] require the loop and subsequently the compensator transfer functions to have a slope of $-12(1 - y)$ dB/octave, where y is phase margin divided by 180 deg. Thus, when the desired phase margin is 120 deg (i.e., $y = 2/3$), the compensator transfer function must have a slope of -4 dB/octave.

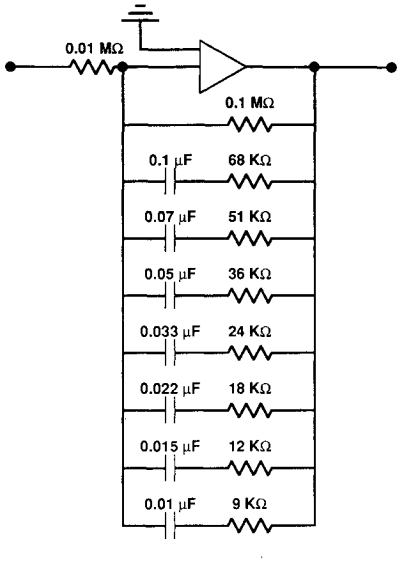

Fig. 9 Compensator schematic.

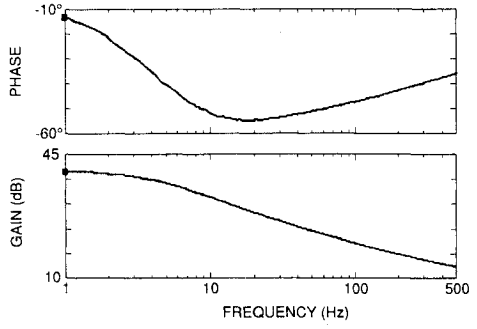

Fig. 10 Measured compensator frequency response function.

To exactly realize such a transcendental transfer function, the compensator needs to be implemented by a system with distributed resistance and capacitance. In this study, the desired compensator frequency response was approximated by transfer function having a finite number of alternating real poles and zeros. Such a compensator was realized with an operational amplifier having seven resistor/capacitor parallel branches in the feedback path as shown in Fig. 9. The resistor and capacitor values were chosen in such a way that the first pole was placed near 5 Hz, and the span between the subsequent poles is about one octave. The resulting compensator frequency response is shown in Fig. 10. The measured maximum phase lag is -55 deg near 20 Hz.

Given this compensator design, the design process was reduced to the determination of the Z' constant that maximized the damping performance. Because of the limited number of active members in this experimental study, the performance goal was limited to the damping augmentation in the first and second truss bending modes only. Without resorting to a formal optimization technique, a direct, iterative search of Z' for best damping performance was employed. To begin with, an initial trial value of Z' was estimated from the averaged load impedance calculated via the finite element analysis such as the one described in Ref 12. Subsequently, the value of Z' could be varied incrementally while comparing the resulting damping performances. It typically required less than ten iterations to reach the final Z' for best damping performance.

As the value of Z' is varied, it is interesting to note that the pure velocity and pure force feedback are the extreme cases of the bridge feedback when the Z' is set to zero and infinity, respectively. With the same range of loop gain coefficients, comparisons on the effect of pure velocity, pure force, and bridge feedback for active member no. 5 are shown in Fig. 11. In Fig. 11a, the increase in loop gain coefficient of the active member with pure velocity feedback is seen to have very little effect on the closed-loop performance. This is due to a near pole/zero cancellation in the loop transfer function resulting from sensing and feeding back what the active member is commanding.[13,14] On the other hand, better closed-loop performance of the active member with pure force feedback is shown in Fig. 11b. However, after the loop gain coefficient passes certain critical value, some of the closed-loop performances such as the eigenvalues of first bending mode in horizontal plane (i.e., $1B_y$) and second bending modes (i.e., $2B_y$ and $2B_z$) start to deteriorate as indicated by the reversed loci. With bridge feedback, Fig. 11c, optimal closed-loop performance is achieved as the root-loci proceed leftward without reversal in the complex plane as the loop gain coefficient increases.

Test Procedure

All of the test data were taken in the form of transfer functions generated by a step sine-sweep test procedure (i.e., a series of sine dwell tests with automated response calculations and frequency increment). To begin with, respective load impedances (i.e., Z_L) facing each active member were measured. For this purpose, active members were actuated one at a time. When an active member was actuated to excite the test structure, transfer functions of its collocated axial force and relative displacement responses were calculated with respect to its driving voltage. Transfer function of the relative velocity response was then obtained by performing differentiation in the frequency domain (i.e., multiplying the displacement response by $j\omega$ where $j = \sqrt{-1}$). Following the convention defined in this paper, the load impedance facing the actuating active member was then estimated by dividing the relative velocity response with the axial force response. The above procedure was then repeated for the other active members.

To characterize the impedance of the active member itself, a similar step sine-sweep test was performed except that the

Table 3 Comparison of open-loop and closed-loop characteristics

Mode no.	Open loop ω, Hz	Open loop ζ, %	Closed loop[a] ω, Hz	Closed loop[a] ζ, %	Closed loop[b] ω, Hz	Closed loop[b] ζ, %	Closed loop[c] ω, Hz	Closed loop[c] ζ, %	Mode description
1	17.74	0.38	17.55	2.22	17.25	4.48	16.69	6.00	1st z bending
2	29.58	0.20	29.50	3.92	28.12	8.00	27.90	10.00	1st y bending
3	33.96	0.38	33.84	0.70	33.72	0.55	33.67	0.71	1st torsion
4	45.10	0.30	44.70	2.00	44.38	2.48	43.40	4.00	2nd z bending
5	65.95	0.17	——[d]	(high)	64.50	3.00	——[d]	(high)	2nd y bending
6	68.43	0.13	68.05	0.31	68.43	0.14	68.05	0.46	2nd torsion

[a]Only active member no. 30 was activated for feedback control.
[b]Only active member no. 5 was activated for feedback control.
[c]Both active members nos. 5 and 30 were activated for feedback control.
[d]Modes are no longer present in transfer functions.

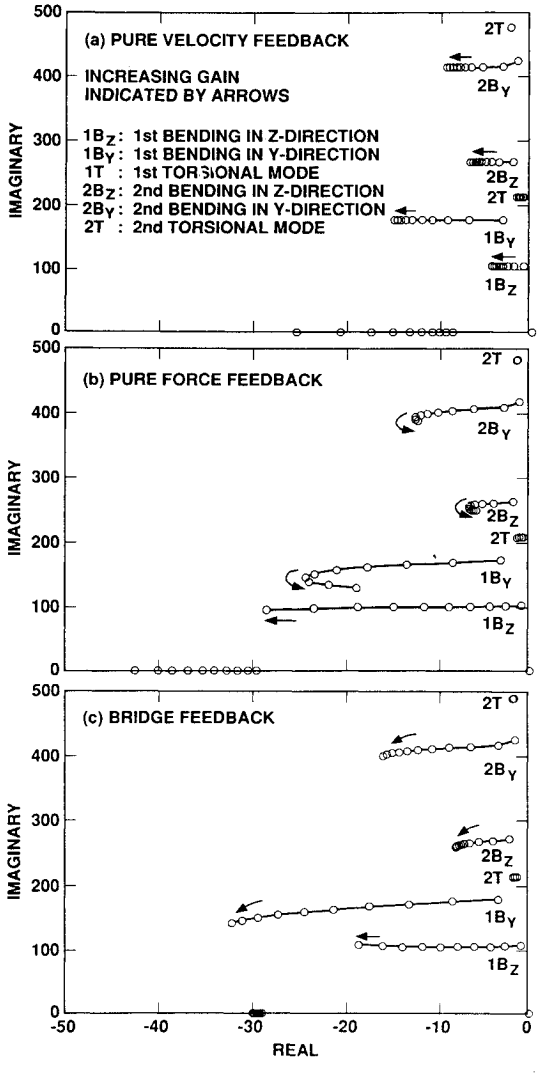

Fig. 11 Comparison of pure velocity, pure force, and bridge feedback control.

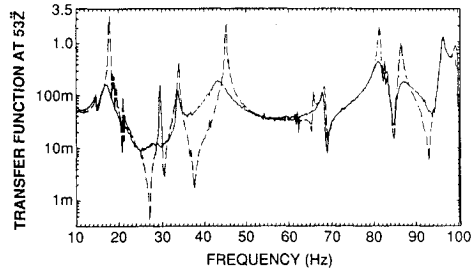

Fig. 12 Comparison of open-loop and closed-loop transfer functions at 34y.

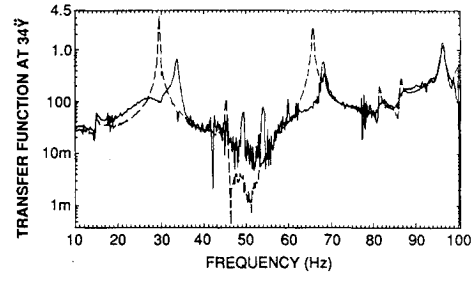

Fig. 13 Comparison of open-loop and closed-loop transfer functions at 53z

test structure was now excited by the mini-shaker attached at joint 23. In this case, all of the transfer functions were calculated with respect to the driving force exerted by the mini-shaker. Each active member's impedance was then found as the ratio of its collocated relative velocity to axial force responses resulting from the mini-shaker excitation. Meanwhile, transfer functions of six accelerometer responses representing the test structure's dynamic behavior were also acquired from the same test. This test was first performed when all of the active members were in open loop. It was then repeated for the three closed-loop cases, i.e., active member no. 5 in closed loop, active member no. 30 in closed loop, and both active members in closed loop.

Results and Discussions

The measured load impedance Z_{L5} facing the active member no. 5 is shown in Fig. 8. As expected, the load impedance is highly frequency dependent due to the dynamics of the test structure. Superimposed in Fig. 8 is the measured impedance of active member no. 5 in open-loop condition, i.e., $Z_{5\ \text{open loop}}$. It is shown that $Z_{5\ \text{open loop}}$ varies by an approximate factor of 10 over the frequency range from 10 to 100 Hz, (i.e., 20 dB/decade). This result agrees with the fact that the impedance of an active member in open-loop condition is dominated by its inherent mechanical stiffness, i.e., s/K.

In Fig. 8, it is also shown that the open-loop active member impedance is orders of magnitude smaller than the load impedance, i.e., $|Z_{5\ \text{open loop}}| << |Z_{L5}|$. This is consistent with the truss structure's design requirement in which the active member's structural stiffness (represented by its axial resonant frequency) is always orders of magnitude higher than the truss structure's system stiffness (represented by the fundamental frequency of the truss structure).

Also included in Fig. 8 is the measured impedance of active member no. 5 in closed-loop condition, i.e., $Z_{5\ \text{closed loop}}$. Instead of rendering a constant impedance as designed in the previous section, $Z_{5\ \text{closed loop}}$ is shown to vary by an approximate factor of 2.5 over the frequency range from 10 to 100

Hz. Such discrepancy is believed to be caused by not having the sufficiently large feedback as assumed in Eqs. (7) and (8). In Fig. 8, the magnitude of $Z_{5\ \text{closed loop}}$ is now increased by an order of magnitude approaching the load impedance. Using the analogy defined in Table 1, the increased $Z_{5\ \text{closed loop}}$ implies that the active member has been dynamically "softened" to "match" its load impedance for better damping augmentation.

Comparison of the measured open-loop and closed-loop transfer functions are shown in Figs. 12 and 13 for accelerometer locations 34y (joint no. 34 in y direction) and 53z, respectively. Modal frequencies and damping values extracted from these transfer functions using a global curve-fitting algorithm are listed in Table 3. For the test configuration investigated in this paper, a 10% modal damping was achieved for the first bending mode in the y direction, while the second bending mode near 66 Hz was completely suppressed as shown in Figs. 12 and 13. Meanwhile, moderate damping performance, i.e., 4–6% modal damping, was achieved for the bending modes in the z direction. Because of the locations of the active members, as expected, no noticeable effect is observed on the damping performance of the first and second torsional modes. In the 34y response, Fig. 12, the closed-loop test result (solid line) shows an additional peak near 33 Hz that does not exist in the open-loop test result (dash line). This peak is identified to be associated with the first torsional mode which is not targeted for control by active member at longeron locations. It is believed that the mode shape of this torsional mode is somewhat modified and shows up in the 34y accelerometer measurement direction as a result of closed-loop control.

Conclusions

Adjusting active member impedance with respect to the load impedance facing the active member provides a powerful way of augmenting vibration damping in a truss-type structure. For a lightly damped structure, the optimal active member impedance should be real and equal to the magnitude of load impedance. Since the load impedance is typically frequency-dependent and sensitive to the structure's parameter variations, an approach to implementing a constant active member impedance over the frequency range of interest was proposed and demonstrated. From an implementation point of view, although not optimal, the constant active member impedance is a desirable feature, for it does not require precise knowledge of the structure's dynamic characteristics that is usually an indispensable requirement for most of the structural vibration control approaches. The use of the bridge feedback concept makes it possible to implement the desired active member impedance without interfering with the compensator design and subsequently the desired loop transfer function.

Appendix: Effect of Feedback on Impedance

The effect of feedback on impedance in an electrical circuit was described by Blackman[15] in 1943. The alternative proofs of the Blackman's result have been published in Refs. 7 and 8. In the following, the effect of feedback on the active member impedance is derived following the logic of Blackman's proof. Considering an active member with feedback as shown in Fig. 3, the relative velocity across the active member $\dot{x}$ and the feedback return signal v can be each expressed as a linear function of the applied force f to the active member and the input signal E to the active member actuator:

$$\dot{x} = a \cdot E + b \cdot f, \qquad v = c \cdot E + d \cdot f \tag{A1}$$

where a, b, c, and d are the constants to be determined from boundary conditions. First, considering the case without feedback, i.e. $E = 0$, gives $\dot{x} = b \cdot f$. Thus, the active member impedance without feedback, Z_0, becomes

$$Z_0 = \dot{x}/f = b \tag{A2}$$

When the loop is closed around the active member, i.e., $E = v$, Eq. (A1) gives $\dot{x} = [b + a \cdot d/(1 - c)] \cdot f$ such that the active member impedance after feedback, Z, becomes

$$Z = b + a \cdot d/(1 - c) \tag{A3}$$

The return ratio T of the active member feedback loop is defined as the ratio of return signal to input signal taken with the opposite sign, i.e., $T = -v/E$. When the active member is rigidly constrained, there is no resulting motion, i.e., $\dot{x} = 0$. In this case, Eq. (A1) gives $f = -a/b \cdot E$ and $v = (c - a \cdot d/b) \cdot E$. Hence, the return ratio T_0 becomes

$$T_0 = -c + a \cdot d/b \tag{A4}$$

On the other hand, when the active member is free to expand, no force is induced in the active member, $f = 0$, so that $v = c \cdot E$ and the return ratio $T\infty$ is

$$T_\infty = -c \tag{A5}$$

Comparing Eqs. (A2–A5) results in the formula of Blackman as

$$Z = Z_0[(1 + T_0)/(1 + T_\infty)] \tag{A6}$$

This formula expresses active member impedance after feedback, Z, in terms of three functions, Z_0, T_0, and T_∞, that do not depend on the structural system to which the active member is connected.

Acknowledgment

The authors wish to acknowledge the assistance of T. Pham, C. Lawrance, and J. McGregor in the laboratory. The research described in this paper was carried out by the Jet Propulsion Laboratory, California Institute of Technology, under a NASA contract.

References

[1]Soosaar K. (ed.), *Passive and Active Suppression of Vibration Response in Precision Structures: State of the Art Assessment*, Vols. 1 and 2, R-1138, Charles Stark Draper Lab., Cambridge, MA, 1978.

[2]Molloy, C. T., "Use of Four-Pole Parameters in Vibration Calculations," *Journal of Acoustical Society of America*, Vol. 29, No. 7, 1957, pp. 842–853.

[3]Crafton, P. A., *Shock and Vibration in Linear Systems*, Harper & Brothers, New York, 1961.

[4]Church, A. H., *Mechanical Vibration*, 2nd ed., Wiley, New York, 1963.

[5]Karnopp, D., and Rosenberg, R., *System Dynamics: A Unified Approach*, Wiley, New York, 1975.

[6]Neubert, V., *Mechanical Impedance: Modelling/Analysis of Structures*, Jostern Printing and Publishing, State College, PA, 1987.

[7]Bode, H. W., *Network Analysis and Feedback Amplifier Design*, Van Nostrand, New York, 1945.

[8]Lurie, B. J., *Feedback Maximization*, Artech House, Dedham, MA, 1986.

[9]Lurie, B. J., "Multiloop Balanced Bridge Feedback in Application to Precision Pointing," *International Journal of Control*, Vol. 51, No. 4, 1990, pp. 785–799.

[10]Lurie, B. J., "Active Damping of Flexible Structures," Jet Propulsion Lab., Engineering Memorandum 343-1207 (Internal Document), Pasadena, CA, Oct. 1990.

[11]Fanson, J. L., Lurie, B. J., O'Brien, J. F., and Chu, C.-C., "System Identification and Control of The JPL Active Structure," AIAA Paper 91-1231, April 1991.

[12]Chen, G.-S., Lurie, B. J., and Wada, B. K., "Experimental Studies of Adaptive Structures for Precision Performance," AIAA Paper 89-1327, April 1989.

[13]Fanson, J. L., Blackwood, G. H., and Chu, C.-C., "Active Member Control of Precision Structures," AIAA Paper 89-1329, April 1989.

[14]Bronowicki, A. J., Mendenhall, T. L., and Manning, R., *Advanced Composite with Embedded Sensor and Actuator*, Interim Rept., AFAL TR-89-086, Edwards AFB, April 1990.

[15]Blackman, R. B., "Effect of Feedback on Impedance," *Bell System Technical Journal*, No. 3, 1943.